

THARSIS MONTES ICE SHEET MODELS AT HIGH OBLIQUITY DRIVEN BY GCM RESULTS. J. L. Fastook¹, J. W. Head², and D. R. Marchant³, ¹Climate Change Institute, University of Maine, Orono, ME 04469 USA (fastook@maine.edu), ²Dept. of Geological Sci., Brown University, Box 1846, Providence, RI 02912 USA (James_Head@Brown.edu), ³Dept. Earth Sci., Boston University, Boston MA 02215 USA (marchant@bu.edu).

Introduction: Fan-shaped deposits on the flanks of the Tharsis Montes volcanoes [1-3] have been interpreted to be glacial in origin, and are likely Amazonian in age [4]. The deposits contain three distinct facies [5], each of which can be associated with different glacial processes [1]. Earth analogs to these three facies have been identified in the Dry Valleys of Antarctica and their climatic implications described [6-7].

In previous work we have shown that fundamental differences between the atmospheric snow accumulation environments on Earth [8] and Mars [9-10], combined with the University of Maine Ice Sheet Model (UMISM) [8,11-12] constrained by geological observations [1-5], allowed us to characterize the mass balance of the Martian ice sheet by two equilibrium lines, and that glacial accumulation is favored on the flanks of large volcanoes, not their summits as seen on Earth. In addition, we have shown that coupling this mass balance parameterization to sample spin-axis obliquity histories [13-14] leads to chronologically reasonable glacial episodes with a maximum configuration that is in accord with the geological observations [15]. However, we found this to be true only for repeated advance and retreat during multiple 100 Ka obliquity cycles where the mean value is in excess of 45°.

In our past reconstructions, we used UMISM constrained by the geological record to define the parameterization of mass balance. While this approach gave a good fit to the geologic record, it yielded little information about how the atmospheric circulation of Mars was actually changing during the periods of high obliquity. In this contribution we describe the use of results from a focused run of an atmospheric general circulation model (GCM) for Mars at high obliquity [16-17]. This GCM, run for a high-obliquity climate, favors deposition of snow on the northwest flanks of the Tharsis Montes due to upwelling and adiabatic cooling of moist polar air as it rises up the slopes of the volcanoes. Predicted, rather than parameterized, accumulation rates are used to drive UMISM, and the resulting ice sheets are compared to the geological evidence. This allows us to assess the validity of the GCM results, and also to assess both the spatial geometry in terms of areal extent and ice volume, and the temporal response in terms of how long such a high obliquity climate must exist to create ice sheet imprints that are in agreement with observed landforms.

Modeling: UMISM uses the well-tested shallow-ice approximation [8,11-12], which is suitable for modeling

ice sheets on Mars because the cold temperatures and low accumulation rates make wet-bed sliding unlikely. In the shallow-ice approximation, a combination of mass and vertically-integrated momentum conservation yields a time-dependent partial differential equation for the ice thickness that requires as source the net mass balance (the difference between a positive deposition of ice and any negative removal over an annual cycle) at each point in the domain. In this simulation, the mass balance distribution is obtained from the results of a GCM run for a high-obliquity climate.

Mass Balance Distribution: The GCM used was the Martian Global Climate Model of the Laboratoire de Meteorologie Dynamique [18-19], a well-tested model able to adequately simulate present Martian climate. A high-obliquity climate was simulated for 45 degrees obliquity (near the most probable value of 41.8 [13]) with a spatial resolution of approximately 2 degrees. The simulation showed net accumulation of 30-70 mm/yr on the western flanks of Olympus, Ascreus, Arsia, and Pavonis Montes, largely due to adiabatically cooled westerlies blowing upslope. The model was relatively insensitive to obliquity, as long as it was greater than 40 degrees, but mildly sensitive to atmospheric dust load, an unknown at high obliquity.

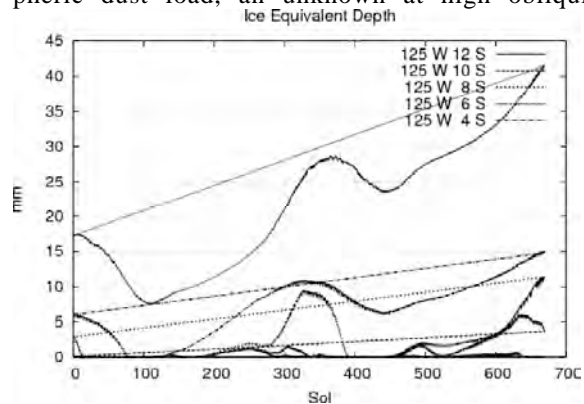


Figure 1: Ice-equivalent depth as a function of Sol.

The GCM results yield ice-equivalent depth (IED) as a function of Sol (Fig. 1). We can use this to separate positive accumulation from negative sublimation in our quest for the net mass balance at each point. For each point the IED may rise and fall throughout the year. As it rises, we sum up total annual accumulation (Fig. 2a), and as it falls, we sum up total annual sublimation (Fig. 2b). The difference represents the net annual mass balance, which is needed for the source in UMISM (Figure 3a). By separating these two components of the mass balance, we allow ourselves the opportunity to shift the

balance between accumulation and sublimation. For instance, we generated Fig. 3a by scaling sublimation by a factor of two to more closely match the geologic record. This method also allows for the specification of a “climate knob” that can be connected to signals such as obliquity variations. Also generated by the GCM and required as an input boundary condition for UMISM is the surface temperature at each point in the domain (Fig. 3b).

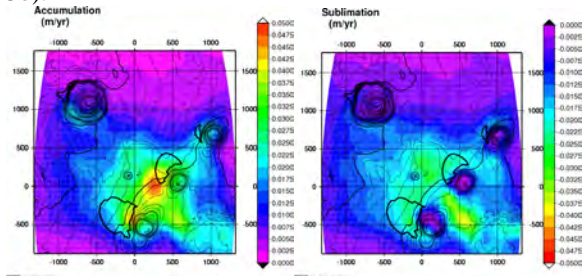


Figure 2: (a:left) Ice-equivalent Accumulation, (b:right) Ice-equivalent Sublimation.

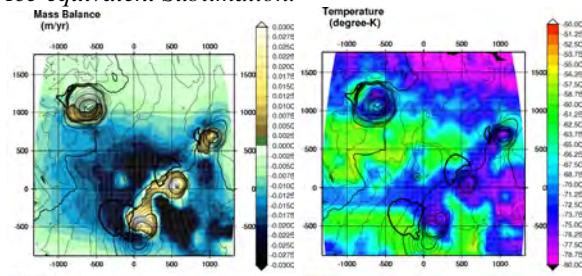


Figure 3: (a:left) Ice-equivalent Net Mass Balance, and (b:right) Surface Temperature.

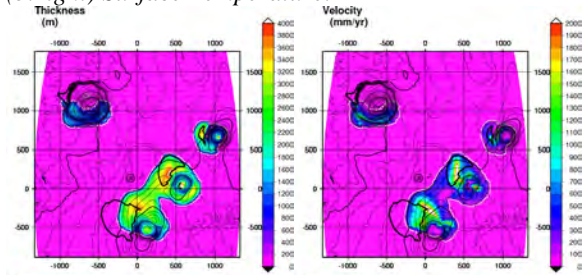


Figure 4: (a:left) Ice Thicknesses and (b:right) Velocities with surface elevations after 500 Ka.

Simulations: The simulation uses constant, fixed input (mass balance and surface temperatures) from the GCM. Figs. 4a,b show the ice thicknesses and column-averaged flow velocities with surface elevations superimposed as contours at the end of 500 Ka of model time. While artificial in the sense that these fixed climatic conditions likely did not hold steady for more than a 100 Ka, the resulting pattern of glaciation is compelling. Approach to steady state is indicated in Fig. 5, showing volume as a function of time. Interestingly, the volume attained after 500 Ka is within 15% of the estimate for the volume of the North Polar Ice Cap,

which in the GCM is the source of moisture for the Tharsis precipitation. The ice thicknesses and velocities (Figs. 4a,b) show moderate agreement with [1]. The Olympus ice sheet is too large and extends too far to the south. The Arsia ice sheet extends too far up the flanks and at the same time does not go far enough to the west. The Pavonis ice sheet engulfs its peak, but matches the northern margin well. Also, the area of maximum velocity where the geologic imprint would be strongest matches the deposits. The Ascreus ice sheet, while slightly too large and with some ice on the peak, matches the deposits reasonably well.

Given the extraordinary topographic relief (> 20 km) of features with lateral extents of just a few hundreds of km, and that the resolution of the simulation is ~15 km, while that of the GCM is ~120 km at the equator, these results are in remarkably close agreement. A very good Earth-based GCM, Polar MM5 [20], produces a mass balance distribution that would yield similar inconsistencies with the current Greenland Ice Sheet, especially along its margin.

We are currently using a variety of predicted spin-axis obliquity histories [13] during the period when the glacial deposits were forming [2-4] to further refine our understanding of the history of the Tharsis tropical mountain glaciers.

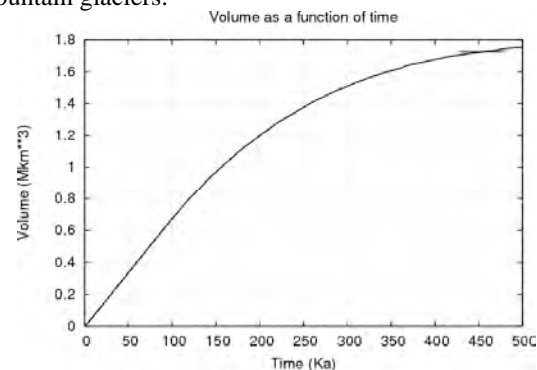


Figure 5: Volume in millions of km^3 versus time.

References: [1] Head, J.W. and Marchant, D.R.. (2003) *Geology*, 31:641-644. [2] Shean, D.E., et al. (2005) *JGR*, 110. [3] Shean, D.E., et al. (2004) *LPS XXXV*, Abstract #1428. [4] Shean, D.E. et al. (2006) *LPS XXXVII*, Abstract #2092. [5] Scott, D.H. and Zimbelman, J.R. (1995) Map I-2480, U.S. Geol. Surv. Misc. Invest. Ser. [6] Marchant, D.R. and Head, J.R. (2004) *LPS XXXV*, Abstract #1405. [7] Marchant, D.R. and Head, J.W. (2005) *LPS XXXVI*, Abstract #1421. [8] Fastook, J.L. and Prentice, M. (1994) *J. Glac.*, 40(134):167-175. [9] Fastook, J.L., et al. (2004) *LPS XXXV*, Abstract #1352. [10] Fastook, J.L., et al. (2005) *LPS XXXVI*, Abstract #1212. [11] Fastook, J.L. (1993) *Computational Science and Engineering*, 1:55-67. [12] Huybrechts, P., et al. (1996) *Annals of Glaciology*, 23:1-12. [13] Laskar, J., et al. (2004) *Icarus*, 170:343-364. [14] Laskar, J., et al. (2004) *LPS XXXV*, Abstract #1600. [15] Fastook, J.L., et al. (2006) *LPS XXXVII*, Abstract #1794. [16] Haberle, R.M., et al. (2004) *LPSC XXXV*, Abstract #1711. [17] F. Forget, et al. (2006) *Science*, 311:368-371. [18] Hourdin, F, et al. (1993) *J. Atmos. Sci.*, 50:3625-3640. [19] Forget, F, et al. (1999) *JGR*, 104:155-176. [20] Box, J.E. et al. (2004) *JGR*, 9:D16105.